

Theory of the heat of solution of hydrogen in Al and Mg using nonlinear screening*

Z. D. Popović[†]

Department of Metallurgy and Materials Science, McMaster University, Hamilton, Ontario, Canada

M. J. Stott

Department of Physics, Queen's University, Kingston, Ontario, Canada

J. P. Carbotte

Department of Physics, McMaster University, Hamilton, Ontario, Canada

G. R. Piercy

Department of Metallurgy and Materials Science, McMaster University, Hamilton, Ontario, Canada

(Received 26 February 1975)

A theory of the heat of solution of hydrogen in simple metals is developed and results are presented for the cases of aluminum and magnesium. The electronic contribution to the heat of solution is treated within the framework of local pseudopotential theory and is based on linear screening. For the proton contribution it is necessary to use nonlinear theory for the screening of the proton and a convenient framework for this is the density functional formalism with exchange and correlation corrections included approximately. The calculated value of the heat of solution for aluminum is 0.45 eV which compares favorably with the experimental value of 0.66 eV. The result for magnesium, -0.05 eV, is also in reasonable agreement with the experimental value of 0.25 eV bearing in mind that the hydrogen heat of solution is obtained as the difference of two energies of about 15 eV. The energy has also been investigated as a function of the position of the proton in the lattice. Calculated energy barriers are used to estimate proton diffusion parameters.

I. INTRODUCTION

Most simple metals dissolve hydrogen only in very small quantities. For example, the metals which are the subject of this investigation, namely Mg and Al, dissolve about 700 parts per million atomic and 1 (ppma), respectively, of hydrogen at atmospheric pressure near their melting points. In spite of the small quantities dissolved, hydrogen in metals is of practical interest because of problems that arise in manufacturing processes. One example is the formation of gas bubbles in the metal after solidification due to dissolved hydrogen.¹ In the case of Al, bubbles form near the surface and lead to blistering.

Hydrogen-metal systems are also of interest because hydrogen is dissociated upon solution and leads to the simplest possible impurities. The H^+ ion, the proton, is a point charge for our purposes with no complicating core electron structure. However, from a theoretical point of view, there are difficulties in treating this impurity because the proton-electron interaction is very strong and cannot be substituted by a weak potential with the same scattering properties. This replacement is the foundation of the pseudopotential method which allows us to treat the properties of simple metals by perturbation theory.

Apart from the relevance to hydrogen-metal systems, the behavior of a heavy particle with unit positive charge in a metal is also relevant to the

positive μ meson which has recently been used as a solid-state probe.² The μ meson with a mass of about 200 electron masses will interact with the ions and electrons of a metal in an identical way to the proton and will differ only in its vibration motion. Apart from negligible effective-mass corrections, the heats of solution, migration energies for diffusion, and the like will be the same for the proton and positive μ meson, but an important difference will be the larger effective jump frequency of the μ meson. The diffusion coefficient for the μ meson will be larger than for the proton by a factor of about $(M_p/M_\mu)^{1/2} \approx 3$.

In an earlier paper, Popović and Stott³ calculated the migration energies for diffusion of hydrogen in Al and Mg using nonlinear-response theory to obtain approximately self-consistent electron densities around the proton. The results for Al were in good agreement with experiment. Experimental data for Mg were not available. A particularly interesting point arising from this investigation was the possibility of hydrogen trapping by vacancies in Al. The energy with the proton at a substitutional site was calculated to be considerably lower (1.23 eV) than with the proton at the most favorable interstitial site. It was proposed that a proton and a μ^+ in metals may behave in a similar way to a positron for which trapping at vacancies, dislocations, voids and, in general, regions of low ion density, in some metals is well documented.

The heat of solution is another basic quantity of interest in a study of hydrogen-metal systems. The only theoretical work on this problem that we are aware of was reported by Friedel,⁴ who treated hydrogen in copper. We will discuss this work fully in a later section. An important ingredient in the theory of the heat of solution is the screening of a proton in the electron gas. Friedel⁴ tackled this problem by trying to solve a set of single-particle Schrödinger equations self-consistently. The screening of a proton in an electron gas has also been treated using linear-response theory.⁵ It is clear from the large electron density near a positron in the electron gas,⁶ as evidenced by the enhanced positron annihilation rate in metals, and a comparison of linear and nonlinear response for the electron density around repulsive point ions,⁷ that the electron-proton interaction is too strong to be treated adequately using linear-response theory.

The density-functional formalism developed by Hohenberg and Kohn⁸ and Kohn and Sham⁹ provides the basis for the investigation of the screening of a proton presented here, and the availability of fast, large-capacity computers has made tractable self-consistent, nonlinear-response calculations of the screening cloud around a proton.

Even though linear-response theory is inadequate for describing the screening of a proton in a metal, it is convenient to develop first of all the linear-pseudopotential theory of the heat of solution. The reason for this is that dissolving a hydrogen atom in a metal involves two particles, an electron and a proton. Consequently, there will be two contributions to the heat of solution. The electron contribution can be calculated with reasonable confidence using pseudopotential theory. The terms representing the proton contribution can then be corrected using the results for the nonlinear screening of the proton. Since pseudopotential theory is used in calculating the electron contribution, the scope of the method is limited to the so-called simple metals. Detailed calculations have been performed for the cases of hydrogen in aluminum and magnesium, and in both of these cases the heat of solution has been measured.

Before proceeding with the detailed theory some general arguments will be presented that will simplify the formulation. First, the heat of solution will not depend on the change in volume of the sample so long as the concentration of hydrogen is small. The argument is similar to that for the case of a vacancy in a metal¹⁰ and will not be repeated here. This allows the assumption of constant-volume conditions to be made in the calculations. Second, the heat of solution will not depend on the state of the metal surface. The spilling out of electrons from the surface of a metal

produces a surface dipole potential which is a major contribution to the electron work function.¹¹ The magnitude of the surface dipole potential is sensitive to the purity and general state of the metal surface, but since the hydrogen atom to be dissolved is electrically neutral there will be no change in energy, due to the surface dipole, as it passes through the surface.

The experimental heat of solution, which is obtained as the slope of the logarithmic plot of the solubility versus $1/T$ at constant hydrogen pressure, is equal to the change in energy of a hydrogen atom dissolved in the metal compared with the energy per hydrogen atom in a hydrogen molecule. To create a free electron and proton from the hydrogen molecule, 2.26 eV per atom is required first of all to dissociate the molecule, and then the atom must be ionized which costs a further 13.60 eV, amounting to a total of 15.86 eV for the process. The observed hydrogen heat of solution ΔH_H will be

$$\Delta H_H = 15.86 + \Delta H_{e1-p}, \text{ eV}, \quad (1)$$

where ΔH_{e1-p} is the heat of solution for a free electron and proton from vacuum, and it is this latter quantity that will be calculated.

The heat of solution is measured at high temperatures, but the small value of about 6×10^{-2} eV for the proton zero-point energy, using the vibrational frequencies estimated in Sec. VII, indicates that it is a good assumption to neglect the motion of the proton and perform the calculations for a rigid arrangement of the ions. It is further assumed that the proton resides at the octahedral site in both aluminum and magnesium. The energy for different positions of the proton has been investigated, and the results justify this assumption with certain reservations in the case of aluminum. Lattice relaxations about the proton have been neglected. A comparison can be made with the case of vacancies in aluminum¹⁰ and magnesium¹² for which the calculated relaxation energies are about -0.03 eV. The forces acting on neighboring ions due to the proton, calculated using the results for the screened electrostatic potential, are of the same order as in the case of a vacancy and, consequently, the relaxation energies cannot be very different. In refinements of the theory it will certainly be desirable to take account of lattice relaxation, and this can be done using standard lattice statics techniques.¹³

When lattice relaxations are neglected it is straightforward to calculate the energy of the system for different positions of the proton. Popović and Stott³ estimated the maximum height of the energy barrier for the proton jumping from one to a neighboring interstitial site, and compared these with experimentally determined activation ener-

gies for diffusion. Additional details of the migration energy barriers will be presented in this paper, and vibrational frequencies of the proton will be estimated. A comparison will be made with the results for activation energies calculated using linear screening for the proton.

The theory of the hydrogen heat of solution will commence with a review of local-pseudopotential theory in Sec. II. Section III is devoted to the linear-pseudopotential theory of the heat of solution, regarding the proton as a point charge with the form factor

$$W_H(\vec{q}) = -4\pi/\Omega_0 q^2. \quad (2)$$

(Atomic units are used throughout with $\hbar = m = e = 1$. The unit of energy is 27.26 eV and the unit of distance is the Bohr radius, 0.529 Å.) Section IV describes the necessary corrections to the heat of solution due to the nonlinear screening of the proton. In Sec. V the density-functional formalism is used to treat the nonlinear screening of a proton in the electron gas, and the method used to obtain an approximate self-consistent solution is described in Sec. VI. In Sec. VII the energy barriers for proton diffusion are calculated. Conclusions are drawn and further applications of the theory are discussed in Sec. VIII.

II. PSEUDOPOTENTIAL THEORY—TOTAL CRYSTAL ENERGY

A local pseudopotential $W(\vec{r})$ which is a simplified Heine-Abarenkov model potential is used for the electron-ion interaction in the calculations. If Z is the valence,

$$W(\vec{r}) = \begin{cases} -ZD/R_m, & r < R_m, \\ -Z/r, & r > R_m, \end{cases} \quad (3)$$

where the core radius R_m , and D , which determines the depth of the potential inside the core, are adjustable parameters.

Following Harrison¹⁴ the total energy V^T of N pseudoions immersed in an electron gas calculated to second order in perturbation theory may be expressed as the sum of three terms

$$V^T = N(ZV_{e1} + V_e + V_b). \quad (4)$$

In Eq. (4), V_{e1} is the energy per electron for the uniform, interacting electron gas plus the average value of the electron-ion interaction. It does not depend on the detailed arrangement of the ions, but only on the density. Using the analytic form proposed by Pines and Nozières,¹⁵ V_{e1} may be written

$$ZV_{e1} = Z \left(\frac{1.105}{r_s^2} - \frac{0.458}{r_s} - 0.0575 + 0.0155 \ln r_s + \sum_{\vec{k}} \langle \vec{k} | W | \vec{k} \rangle \right), \quad (5)$$

where $(3/4\pi r_s^3) = (\Omega_0/Z)^{-1} = n_0$ is the mean electron density and Ω_0 is the atomic volume. Introducing the pseudopotential form factor $W(\vec{q})$ given by

$$W(\vec{q}) = \frac{-4\pi Z}{\Omega_0 q^2} \left(\frac{D \sin q R_m}{q R_m} + (1-D) \cos q R_m \right) \quad (6)$$

and appropriate uniform charge backgrounds, so that individual terms in Eq. (4) are finite

$$\sum_{\vec{k}} \langle \vec{k} | W | \vec{k} \rangle = \lim_{q \rightarrow 0} \left(\frac{4\pi Z}{\Omega_0 q^2} + W(\vec{q}) \right). \quad (7)$$

The second term in (4) is the electrostatic ion-ion interaction energy. It can be evaluated using an Ewald method and may be expressed in the form¹⁴

$$V_e = \lim_{\xi \rightarrow \infty} \left[\sum_{\vec{q} \neq 0} |S(\vec{q})|^2 F_e(q) - Z^2 \left(\frac{\xi}{\pi} \right)^{1/2} - \frac{\pi Z^2}{2\xi \Omega_0} \right] \quad (8)$$

where

$$F_e(q) = (2\pi Z^2/\Omega_0 q^2) \exp(-q^2/4\xi)$$

and $S(\vec{q})$ is the structure factor, which is given in terms of the ion position \vec{R}_j by

$$S(\vec{q}) = N^{-1} \sum_j \exp(i\vec{q} \cdot \vec{R}_j). \quad (9)$$

For a perfect crystal,

$$V_e = \alpha Z^5/2r_s, \quad (10)$$

where α is the Ewald constant having the values -1.79175 for the fcc lattice and -1.79166 for the hcp structure.

The last term in (4) is known as the band-structure energy and is given by

$$NV_b = N^{-1} \sum_{\vec{q} \neq 0} |NS(\vec{q})W(\vec{q})|^2 g(\vec{q}). \quad (11)$$

For a local pseudopotential g is given by¹⁶

$$g(\vec{q}) = -\frac{1}{2} \frac{\Omega_0}{4\pi/q^2} \frac{1 - \epsilon^{-1}(\vec{q})}{1 - f(\vec{q})}. \quad (12)$$

The function $f(\vec{q})$, which accounts for exchange and correlation corrections and depends on the mean electron density, also appears in the electron dielectric function

$$\epsilon(\vec{q}) = 1 + [1 - f(q)] \frac{4k_F}{\pi q^2} \left(\frac{1}{2} + \frac{4k_F^2 - q^2}{8k_F q} \ln \left| \frac{2k_F + q}{2k_F - q} \right| \right). \quad (13)$$

In the calculations we have used the parametrized form for $f(\vec{q})$ proposed by Singwi *et al.*¹⁷

Equations (4)–(11) for the total energy are valid for any configuration of identical ions. When all of the ions are not the same the expression must be slightly modified, and this will be carried out in Sec. III for the case of a hydrogen impurity.

The pseudopotential parameters have been chosen so that the observed equilibrium lattice parameter and the binding energy for the perfect crystal are given accurately to second order in perturbation theory using Eq. (4). In previous calculations of the vacancy formation energy and volume,^{18,10} the pseudopotential parameters were fitted to the observed equilibrium lattice condition and bulk modulus. In the case of the heat of solution, the observed binding energy rather than the bulk modulus was felt to be a more appropriate second quantity for the fitting since energies relative to the vacuum level are of interest. The binding energy per atom is merely V^T/N . The equilibrium lattice condition given explicitly to second order by Popović *et al.*¹⁰ is obtained from $(\partial V^T/\partial \delta)_{\delta=0} = 0$, where δ is a uniform dilation. Table I lists the observed lattice parameters, the binding energies, and the deduced pseudopotential parameters for aluminum and magnesium.

III. LINEAR-RESPONSE THEORY FOR HEAT OF SOLUTION

Consider the total energy when a proton and an additional electron are introduced into the metal. The changes in each of the three contributions in Eq. (4) will be considered in turn.

The total electron-gas energy in Eq. (4) (NZV_{e1}) will be modified owing to the introduction of an additional electron. This will change the number of electrons to $NZ+1$ and the Fermi wave vector to $k'_F = k_F(1+1/3NZ)$, giving for the change in energy to order unity

$$\Delta(NZV_{e1}) = V_{e1}(k_F) + \frac{k_F}{3} \frac{\partial V_{e1}(k_F)}{\partial k_F}. \quad (14)$$

Note that the average value of the electron-ion interaction Eq. (7) does not change with k_F because the atomic volume per host ion remains the same.

The electrostatic energy NV_e will change because of the addition of a proton. Since lattice relaxations around the proton are neglected, the change in the total electrostatic energy due to the Coulomb interaction between the proton and the

ions, together with a neutralizing uniform negative background, will be

$$\Delta(NV_{e1}) = \alpha_H Z^{2/3}/r_s. \quad (15)$$

The constant α_H depends on the position of the proton with respect to the ions and the crystal structure. It can be calculated by Ewald's method. Assuming that the proton occupies an octahedral site, $\alpha_H = -0.42586$ for the fcc structure and $\alpha_H = -0.42732$ for the hcp structure, with the c/a ratio appropriate to Mg.

The band-structure energy in Eq. (4) (NV_b) changes owing to the introduction of the proton and the additional electron. In considering this term it is convenient to introduce the set of reciprocal-lattice vectors \vec{K}_n for the fcc lattice in the case of Al and the hexagonal lattice in the case of Mg. In terms of \vec{K}_n , the structure factor for Al can be chosen to be

$$S(\vec{q}) = \sum_n \delta_{\vec{q}, \vec{K}_n}, \quad (16)$$

and for Mg, if $\vec{\rho}_2$ is the position of the second atom in the unit cell,

$$S(\vec{q}) = \frac{1}{2}[1 + \exp(i\vec{q} \cdot \vec{\rho}_2)] \sum_n \delta_{\vec{q}, \vec{K}_n}. \quad (17)$$

Owing to the presence of the proton, $NS(\vec{q})W(\vec{q})$ in Eq. (11) becomes $NS(\vec{q})W(\vec{q}) + W_H(\vec{q}) \exp(-i\vec{q} \cdot \vec{\rho}_H)$, where $\vec{\rho}$ is the position of the proton and k_F changes because of the additional electron. Again, noting that the atomic volume per host ion Ω_0 remains constant, a straightforward calculation yields for the change in the band-structure energy to order unity for the hcp structure

$$\begin{aligned} \Delta(NV_b) = & \frac{k_F}{3Z} \sum_{n \neq 0} \cos^2(\frac{1}{2}\vec{K}_n \cdot \vec{\rho}_2) W^2(\vec{K}_n) \frac{\partial}{\partial k_F} g(\vec{K}_n) \\ & + \sum_{n \neq 0} W(\vec{K}_n) W_H(\vec{K}_n) \{ \cos(\vec{K}_n \cdot \vec{\rho}_H) + \cos[\vec{K}_n \cdot (\vec{\rho}_2 - \vec{\rho}_H)] \} \\ & + N^{-1} \sum_{\vec{q} \neq 0} W_H^2(\vec{q}) g(\vec{q}). \end{aligned} \quad (18)$$

For fcc crystals the result has the same form with $\vec{\rho}_2 = 0$.

Adding up the changes in the energy given by Eqs. (14), (15), and (18), the expression for the heat of solution of ionized hydrogen is obtained,

$$\Delta H_{e1-p} = \Delta H_1 + \Delta H_2, \quad (19)$$

where

$$\begin{aligned} \Delta H_1 = & V_{e1}(k_F) + \frac{k_F}{3} \frac{\partial V_{e1}(k_F)}{\partial k_F} + \alpha_H \frac{Z^{2/3}}{r_s} \\ & + \frac{k_F}{3Z} \sum_{n \neq 0} \cos^2(\frac{1}{2}\vec{K}_n \cdot \vec{\rho}_2) W^2(\vec{K}_n) \frac{\partial}{\partial k_F} g(\vec{K}_n) \end{aligned} \quad (20)$$

depends only on the properties of the perfect crystal, and

TABLE I. Table of lattice parameters, c/a ratio, binding energy per atom, and model-potential parameters for Al and Mg.

	a (Å)	c/a	V^T/N (a. u.)	$k_F R_m$	D
Al	4.031	...	-2.082	1.285	0.3969
Mg	3.193	1.624	-0.855	1.227	0.4507

TABLE II. Results of calculations of proton correlation energy with $r_s = 2.064$ a. u. appropriate to Al. Trial potential parameters and V_{int}/Z_p are given for different values of the charge Z_p on the heavy impurity, calculated using nonlinear Hartree theory and the nonlinear theory with exchange and correlation corrections. The final row lists the resulting proton correlation energies obtained using (26) and the result obtained using linear-response theory.

Z_p	Trial potential parameters		V_{int}/Z_p (a. u.)		
	α	β	Linear theory	Nonlinear (Hartree)	Nonlinear (exch + corr)
0.25	1.101	1.024		-0.194	
	0.899	1.348			-0.220
0.5	1.159	1.001		-0.423	
	0.987	1.290			-0.486
0.75	1.219	0.977		-0.694	
	1.075	1.229			-0.807
1.0	1.273	0.954		-1.016	
	1.153	1.171			-1.186
Proton correlation energy E_{corr} (a. u.)			-0.401	-0.451	-0.522

$$\Delta H_2 = \sum_{n \neq 0} W(\vec{K}_n) W_H(\vec{K}_n) \{ \cos(\vec{K}_n \cdot \vec{\rho}_H) + \cos[\vec{K}_n \cdot (\vec{\rho}_H - \vec{\rho}_2)] \} + N^{-1} \sum_{q \neq 0} W_H^2(\vec{q}) g(\vec{q}) \quad (21)$$

depends upon the presence of the proton through the form factor W_H .

The hydrogen heats of solution for Al and Mg, calculated from Eqs. (1) and (21) using the model-potential parameters listed in Table I, are quoted together with the results of the nonlinear-screening theory in Table V. The hydrogen heat of solutions for Al has been measured by Eichenauer¹⁹ and for Mg by Popović and Piercy,²⁰ and their results are also quoted in Table II. The linear theory is seen to be inadequate giving values that are too large. It also predicts incorrectly that the heat of solution for Mg is larger than for Al.

Linear theory is probably providing an adequate treatment of ΔH_1 since this term does not depend on the screening of the proton, and consequently Eq. (21) underestimates ΔH_2 . In order to obtain better agreement with experiment it is essential to go beyond linear theory in treating the screening of the proton. A self-consistent nonlinear theory of the screening of a proton will be developed in Sec. IV and applied in a more careful treatment of the hydrogen heat of solution.

IV. NONLINEAR CORRECTIONS

The term ΔH_2 in the expression for the heat of solution can be rewritten in a more transparent form so that it is clear how to make corrections that take into account nonlinear screening of the

proton. Equation (21) can be written

$$\Delta H_2 = \sum_{q \neq 0} s(\vec{q}) W(\vec{q}) n^{(1)}(\vec{q}) + \frac{1}{2N} \sum_{q \neq 0} \exp(i\vec{q} \cdot \vec{\rho}_H) W_H(\vec{q}) n^{(1)}(\vec{q}), \quad (22)$$

where $n^{(1)}(\vec{q})$ is the displaced electron density around the proton in an electron gas calculated to first order in W_H , and is given by

$$n^{(1)}(\vec{q}) = 2g(q) W_H(\vec{q}) \exp(-i\vec{q} \cdot \vec{\rho}_H). \quad (23)$$

The first term in Eq. (22) is the interaction energy between the electron screening cloud around the proton and the ions. The second term is the leading term in a perturbation expansion for the electron-proton correlation energy E_{corr} for an electron gas. This correlation energy does not involve the surface dipole potential since the proton is not introduced into the electron gas through an external surface; rather it is the change in ground-state energy as the electron-proton interaction is slowly turned on.

The nonlinear response of the electrons to the presence of the proton can be accounted for by modifying Eq. (22) to read

$$\Delta H_2 = \sum_{q \neq 0} S(\vec{q}) W(\vec{q}) n(\vec{q}) + E_{\text{corr}}, \quad (24)$$

where $n(\vec{q})$, expressed in terms of the displaced density $\Delta n(\vec{r})$ around the proton, is

$$n(\vec{q}) = \int_0^\infty dr 4\pi r^2 \Delta n(\vec{r}) \frac{\sin qr}{qr} \quad (25)$$

The electron-proton correlation energy can be

calculated conveniently by introducing $\Delta n(Z_p, \vec{r})$, the displaced density around a heavy impurity, with electric charge $Z_p e$ where Z_p ranges from 0 to 1. The derivation uses Feynman's theorem and follows precisely that given for the electron-positron correlation energy by Hodges and Stott,²¹ and the result is

$$E_{\text{corr}} = \int_0^1 \frac{dZ_p}{Z_p} \left(- \int d\vec{r} \frac{Z_p}{r} \Delta n(Z_p, \vec{r}) \right), \quad (26)$$

where

$$V_{\text{int}} = - \int d\vec{r} \frac{Z_p}{r} \Delta n(Z_p, \vec{r})$$

is just the electron-proton interaction energy for the charge $Z_p e$. Using Eqs. (24)–(26), corrections to the hydrogen heat of solution taking into account the strong nature of the electron-proton interaction can be made in terms of the displaced electron density around a fractionally charged positive impurity in the electron gas.

V. NONLINEAR PROTON SCREENING

In this section the method used for calculating the screening cloud around a proton and a fractionally charged positive impurity is described and compared with earlier calculations.

The theoretical foundation of the method used here to treat the screening of the proton has been developed by Hohenberg and Kohn⁸ and Kohn and Sham⁹ and is usually referred to as the density functional formalism. Results of the formalism pertinent to this work will now be presented.

The central result of interest is the existence of a one-body local potential $V_{\text{eff}}(\vec{r})$ which, through the one-body Schrödinger equation

$$\left[-\frac{1}{2} \nabla^2 + V_{\text{eff}}(\vec{r}) \right] \psi_i(\vec{r}) = \epsilon_i \psi_i(\vec{r}), \quad (27)$$

generates the set of wave functions ψ_i and energy eigenvalues ϵ_i , from which the exact ground-state density of the system may be obtained using the independent-particle result

$$n(\vec{r}) = \sum_{\epsilon_i < \mu} |\psi_i(\vec{r})|^2, \quad (28)$$

where μ is the electron chemical potential. The effective potential may be expressed in the form

$$V_{\text{eff}}(\vec{r}) = V(\vec{r}) + V_{\text{xc}}(\vec{r}), \quad (29)$$

where $V(\vec{r})$ is the total electrostatic or Hartree potential

$$V(\vec{r}) = V_{\text{ext}}(\vec{r}) + \int d\vec{r}' \frac{n(\vec{r}')}{|\vec{r} - \vec{r}'|} \quad (30)$$

and V_{xc} is the functional derivative of a universal exchange and correlation-energy functional $E_{\text{xc}}[n]$ of the particle density n :

$$V_{\text{xc}}(\vec{r}) = \delta E_{\text{xc}}[n] / \delta n(\vec{r}). \quad (31)$$

Up to this point the scheme for calculating the ground-state density is exact; but in practice, approximations are involved because of an incomplete knowledge of the functional $E_{\text{xc}}[n]$. A realistic approximation for the case of a slowly varying density replaces the nonuniform electron system locally by a uniform electron gas of mean density $n(\vec{r})$, and

$$E_{\text{xc}} \simeq \int d\vec{r} n(\vec{r}) \epsilon_{\text{xc}}(n(\vec{r})), \quad (32)$$

where $\epsilon_{\text{xc}}(n)$ is the exchange and correlation energy per electron for a uniform electron gas of density n ; consequently,

$$V_{\text{xc}}(\vec{r}) \simeq \mu_{\text{xc}}(n(\vec{r})) = \epsilon_{\text{xc}} + \left(\frac{n d\epsilon_{\text{xc}}}{dn} \right)_{n=n(\vec{r})}. \quad (33)$$

$\mu_{\text{xc}}(n)$ is the exchange and correlation part of the electron chemical potential for the uniform electron gas. This approximation has been used, and the parameterized form for μ_{xc} proposed by Hedin and Lundqvist,²² based on the work of Singwi *et al.*,¹⁷ has been adopted for the detailed calculations. In the calculations the zero of potential was chosen so that $V_{\text{eff}}(r) \rightarrow 0$ as $r \rightarrow \infty$.

It is straightforward to apply Eqs. (27)–(33) to the case of a heavy positive particle with charge $Z_p e$ in a uniform electron gas. In view of the spherical symmetry it is convenient to express the single-particle wave function in terms of partial waves $R_{l\mathbf{k}}(r)$ which satisfy the usual radial Schrödinger equation

$$\left(-\frac{1}{2} \frac{\partial^2}{\partial r^2} + V_{\text{eff}}(r) + \frac{l(l+1)}{2r^2} - \epsilon_{\mathbf{k}} \right) r R_{l\mathbf{k}}(r) = 0. \quad (34)$$

For the continuum states $\epsilon_{\mathbf{k}} = \frac{1}{2} k^2$, where \vec{k} is the electron wave vector labelling the states, and the zero of energy is taken to be the potential far from the impurity. S-type bound states sometimes occur, and for these cases the wave functions will be denoted by $R_b(r)$.

Since the impurity must be completely screened at large distances $r V_{\text{eff}}(r) = 0$ as $r \rightarrow \infty$, and the radial wave functions for the continuum states will have the asymptotic form well known from partial-wave analysis

$$R_{l\mathbf{k}}(r) = \cos \eta_l j_l(kr) - \sin \eta_l n_l(kr), \quad (35)$$

where the phase shifts η_l depend on k and j_l and n_l are the spherical Bessel and Neuman functions, respectively. For a bound state with energy $\epsilon_b < 0$, the asymptotic form is

$$r R_b(r) \sim e^{-k_0 r}, \quad (36)$$

where $k_0 = (-2\epsilon_b)^{1/2}$.

The change in density induced by the impurity particle can be expressed in terms of the radial wave functions

$$\begin{aligned}\Delta n(r) &= \sum_{\epsilon_i < \mu} |\psi_i(\vec{r})|^2 - n_0, \\ \Delta n(r) &= \frac{1}{\pi^2} \int_0^{k_F} dk k^2 \sum_{l=0}^{\infty} (2l+1) \\ &\quad \times \{ [R_{l\mathbf{k}}(r)]^2 - j_l^2(kr) \} + 2[R_b(r)]^2,\end{aligned}\quad (37)$$

where R_b is normalized so that

$$\int_0^{\infty} dr 4\pi r^2 [R_b(r)]^2 = 1.$$

The sum over angular momentum quantum numbers l in Eq. (38) converges rapidly. This is because the effective potential is localized so that radial wave functions for large l will differ little from the corresponding unperturbed functions, j_l being dominated by the centrifugal term in Eq. (34).

In order to have complete screening of the impurity the total displaced charge must balance the charge of the impurity. This condition can conveniently be expressed in terms of the phase shifts evaluated at the Fermi level, the result

$$Z_p = \frac{2}{\pi} \sum_{l=0}^{\infty} (2l+1) \eta_l(k_F) \quad (39)$$

is the well-known Friedel sum rule. In applying Eq. (39) account is taken of displaced charge in the form of bound states through the condition $\eta_l(0) = n\pi$, where $2n(2l+1)$ is the number of bound electrons with quantum number l .

The electron-proton correlation energy may be calculated using Feynman's theorem and the displaced density around a positive impurity with charge $Z_p e$, as indicated in Sec. IV. Alternatively it can be calculated by substituting the electron density around the proton into the energy functional of the density. However, the latter method would involve a large degree of cancellation between different terms, particularly between the change in the sum of eigenvalues and the Hartree electrostatic self-energy term. There is no problem of this type in using the coupling-constant method, and so that approach has been used for the calculations.

The scheme described above may be viewed as a nonlinear self-consistent Hartree calculation with approximate corrections for exchange and correlation. However the density functional formalism is in principle exact; it also gives a guide to how exchange and correlation effects should be included and generally places the scheme on a firmer theoretical footing. The self-consistent Hartree method, where the effective potential is

merely given by $V(\vec{r})$ [Eq. (30)], has been used to treat the nonlinear screening of repulsive point ions and the results used to estimate vacancy formation energies.²³

Nonlinear-response calculations of the electron distribution around mobile and fixed point charges in an electron gas have been reported by Sjölander and Stott.⁷ The work of these authors was based on an extension of the theory of an electron gas developed by Singwi *et al.*^{24,17} to a two-component system. The method dealt well with repulsive impurities and gave similar results to the self-consistent Hartree method for heavy impurities, but it proved inadequate for treating the screening of a positron for larger values of r_s and broke down for the proton throughout the metallic range of electron densities. The symptom of this breakdown was an excessive pile-up of charge near to the attractive impurity particle, and since it is the kinetic-energy cost that limits electron localization, it could be this aspect of the problem that is treated improperly in this method. Also the presence of resonant states or actual bound states is not accounted for in the method. The method has since been refined by Bhattacharyya and Singwi²⁵ by taking some account of three-particle correlations, and has been used successfully to treat the positron annihilation rate. These authors also used the method to calculate the electron density around a proton in an electron gas with $r_s = 2$ a. u. close to that adopted here for Al. Their results will be compared with the results for Al presented later in Sec. VI.

The screening of heavy, positively charged impurities is more difficult to treat than the case of the light positron or a repulsive particle because of the possibility of resonances or actual bound states occurring. The most straightforward way to account for these possibilities is to solve exactly an appropriate single-particle Schrödinger equation. A calculation of this type for the case of a proton was first reported by Friedel⁴ who examined the hydrogen-copper system. The starting point of this calculation was a proton with one bound electron which was stabilized by Slater exchange between it and parallel-spin conduction electrons. No valence-valence exchange was included, and there were no correlation corrections. Friedel corrected for the presence of the ions and estimated the hydrogen heat of solution for copper to be 0.2 eV, in reasonable agreement with the recent experimental value of 0.57 eV. Friedel calculated the wave function of the bound electron in the field of the proton and conduction electrons so that at large distances from the proton the bound electron moves in an unscreened Coulomb field, which will give an overestimate of the binding energy and is unrealistic.

The procedure outlined earlier and adopted for the calculations is not directly applicable to spin-polarized screening. However, an exchange-correlation potential for use with a spin-polarized ground state has been proposed by von Barth and Hedin,²⁶ and with substantially more computational effort this case could be investigated. We do not think that the single-bound-electron configuration is relevant to simple metals since, for a high electron-gas density, the random-phase approximation (RPA) should be good and there will be no bound states. And for low electron density, where exchange should be most important, the limiting case will be the ground state of the H^- ion in the Wigner lattice.

VI. APPROXIMATE SELF-CONSISTENT SOLUTION

The formalism described in Sec. V is similar to that used in self-consistent-field calculations for atoms, and it is well known that these converge well; a reasonable trial function after a few iterations yields good self-consistency. The immediate difficulty in the screening of a proton in an electron gas lies in conserving the number of particles and ensuring complete screening at large distances from the proton: for the atom with a relatively small number of electrons this is no problem. The trial potential and any other generated by iteration does not necessarily satisfy the Friedel sum rule and will behave incorrectly, $V_{\text{eff}} \sim 1/r$, at large distances. It might appear appealing to treat the screening problem by considering a finite number of particles in a large box. March and Murray²⁷ have performed such calculations to treat the screening of a pseudoion without attempting self-consistency. They concluded that a prohibitively large number of particles (10^6 or more) would be necessary to make effects due to the box boundary conditions negligible.

A self-consistent solution of Eqs. (34)–(38) was first attempted by starting with a trial potential $V_{\text{eff}}(r) = V_{\text{trial}}(r, \alpha)$ containing a single parameter α which was determined so that the Friedel sum rule, Eq. (39), was satisfied. Using this potential and Eqs. (34)–(38) a new potential was generated and adjusted so that the Friedel sum rule was again satisfied. In spite of many different sorts of adjustments this procedure was not convergent, and in successive iterations the violation of the Friedel sum rule increased.

The procedure finally adopted achieved good self-consistency and started with a two-parameter trial potential, $V_{\text{trial}}(r, \alpha, \beta)$. The parameters α and β were determined so that the Friedel sum rule was satisfied by both the trial potential and the potential generated from it using Eqs. (34)–(39). A number of analytic forms for the trial potential were tried and they all gave very similar

results, the electron-proton correlation energy not differing by more than 0.5% or less than 0.1 eV. A trial function of the form

$$rV_{\text{trial}}(r) = -e^{-\alpha r^\beta} \quad (40)$$

was found to be most flexible since α and β could be chosen to produce the correct Friedel sum rules for any value of Z_p between 0 and 1, with or without exchange and correlation corrections in the potential, for both aluminum and magnesium electron densities.

The details of the computational procedure will now be described systematically. Starting with the trial potential, Eq. (40), with the parameter β fixed, the parameter α was calculated so that the Friedel sum rule was satisfied to high accuracy. The radial Schrödinger equation was solved numerically in steps of 0.05 a. u. out to a radius $R_0 = 10$ a. u. using a method described by Fox and Goodwin²⁸ (method VII). The potential was put to zero for $r > R_0$, the numerical solution matched to the analytic solution given by Eq. (35), and the phase shifts found. The analytic solution was later used for $r > R_0$. Radial wave functions with $0 \leq k \leq k_F$ were required to construct the displaced electron density, Eq. (38), and for the integration over k the Gauss integration formula of the 48th order was used. Seven partial waves were used in the sum over l in Eq. (38). The phase shifts $\eta_0(k_F)$ were very small ($\sim 10^{-4}$) so that little error was introduced by neglecting the changes in wave functions with $l > 6$. In some cases an s -like bound state appears with $\eta_0 \rightarrow \pi$ as $k \rightarrow 0$. The bound-state wave function and energy were found by matching the numerical solution for $r < R_0$ to the asymptotic solution given by Eq. (36) at $r = R_0$. The parameters α and β and the electron-proton correlation energy were changed by less than $\frac{1}{2}\%$ by doubling R_0 , halving the integration interval, or using the 64- rather than 48-point Gauss integration formula. Once the displaced charge is known the new effective potential can be found, for which the Friedel sum is then calculated. This whole procedure is then repeated with an adjusted value of β until the correct Friedel sum is obtained.

Values of the parameters α and β determined in this way for different values of Z_p , together with the corresponding interaction energies and the resulting electron-proton correlation energies, are given in Tables II and III for Al and Mg electron densities, respectively. Results are presented for linear-response theory, the self-consistent nonlinear Hartree approximation, and the full self-consistent nonlinear theory including exchange and correlation.

Linear-response theory underestimates substantially the magnitude of the electron-proton correlation energy. The results for the displaced den-

TABLE III. Results of calculations of proton correlation energy with $r_s = 2.642$ a. u. appropriate to Mg. Trial potential parameters and V_{int}/Z_p are given for different values of the charge Z_p on the heavy impurity, calculated using nonlinear Hartree theory and the nonlinear theory with exchange and correlation corrections. The final row lists the resulting proton correlation energies obtained using (26) and the result obtained using linear-response theory.

Z_p	Trial potential parameters		V_{int}/Z_p (a. u.)		
	α	β	Linear theory	Nonlinear (Hartree)	Nonlinear (exch + corr)
0.25	0.969	1.042		-0.168	
	0.665	1.630			-0.201
0.5	1.046	1.008		-0.373	
	0.811	1.485			-0.455
0.75	1.123	0.976		-0.627	
	0.949	1.355			-0.775
1.0	1.197	0.943		-0.937	
	1.063	1.237			-1.157
Proton correlation energy E_{corr} (a. u.)			-0.344	-0.406	-0.497

sities indicates that this arises from a less pronounced pile-up of electrons near the impurity. Exchange and correlation corrections also play an important role giving considerably lower energies than simple Hartree calculations. The full calculations revealed shallow bound s -states for $Z_p = 1$, with energies approximately 0.005 a. u. for Mg and 0.0005 a. u. for Al. In the case of Mg, the bound electrons contributed 30% of the total electron density at the proton; for Al they contributed only about 10%, which indicates a spatially more extensive bound state for Al compared with Mg, which is consistent with the smaller binding energy. The bound states around the proton should merge with the continuum for larger electron-gas densities than those considered. There were no bound states for the smaller values of Z_p investigated. Hartree screening did not give a bound state for Al and gave but a very shallow one for Mg.

The single-particle eigenstates and in particular the bound state are not relevant to the single-particle excitation spectrum as measured approximately in a soft-x-ray emission experiment or by x-ray photoemission. The density functional formalism as presented earlier deals only with the ground-state energy and particle density. In any case, an experiment involving the excitation of one or more particles could not be used to distinguish between shallow bound s -states or incipient bound s -states in the continuum, because the lifetime of holes deep in the Fermi sea is short, leading to poor energy resolution (a hole near the bottom of the conduction band would be about 1.3 eV wide²⁹).

Table IV presents phase shifts for $k = k_F$ ob-

tained from the calculation including exchange and correlation. For both Al and Mg the rapid decrease of phase shift with increasing l is evident. The large s -wave phase shift also indicates that the scattering at $k = k_F$ is predominantly s wave.

The most dramatic differences between linear- and nonlinear-response theory can be seen in the displaced electron densities around the proton, which are illustrated in Figs. 1 and 2 for Mg and Al, respectively. At the proton site the electron pile-up is about ten times greater than the linear-response result for Mg and about six times for Al. For comparison the electron density in atomic hydrogen is presented. It is smaller than in the metal in the region near the proton, but of the same order of magnitude. The densities calculated using the Hartree method are also presented, and as expected the density near the proton is underestimated. This is because the exchange-correlation hole around an electron, when it is near to the proton, leads to reduced screening of the proton charge and consequently to a more attractive potential than the electrostatic potential without many-body corrections. The electron density at the proton site is roughly four times larger than

TABLE IV. Phase shifts calculated at $k = k_F$ for a proton in a uniform electron gas of mean density appropriate to Al and Mg.

	η_0	η_1	η_2	η_3	η_4	η_5
Al	1.081	0.1210	0.0196	0.0033	0.0005	0.0001
Mg	1.272	0.0796	0.0095	0.0012	0.0000	0.0002

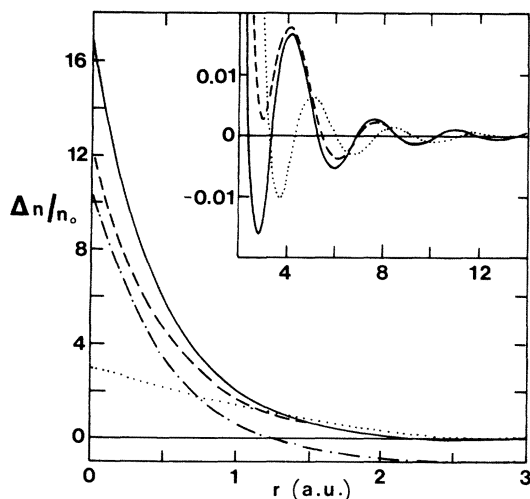


FIG. 1. Displaced electron density, $\Delta n(r) = n(r) - n_0$ in units of n_0 plotted against r (a. u.) for a proton in a uniform electron gas of mean density appropriate to Al ($r_s = 2.064$ a. u.). Results are presented for the nonlinear theory with exchange and correlation corrections (solid line), the nonlinear Hartree theory (dash line), linear response theory (dotted line), and for the hydrogen atom (dash-dot line).

that at a positron in the electron gas. This is because the positron, with the mass of an electron, recoils after a collision, and in the center-of-mass frame the ratio of kinetic-to-potential energy is greater than for the proton, leading to weaker scattering. The electron density varies rapidly near the proton, and the local density approximation for the exchange-correlation potential will probably be poor in this region. Fortunately, near the proton the effective potential will be dominated by the Hartree potential ($V \sim -1/r$), and errors in V_{xc} should not greatly effect the density. However, the approximation used for V_{xc} is certainly the most serious in the whole procedure.

Friedel oscillations in the charge density are clearly exhibited in Figs. 1 and 2. Similar oscillations are present in the Hartree and effective potentials which are not shown. Both nonlinear-response calculations yield density oscillations which are shifted in phase by about 90° from those for linear response. This is an important characteristic of nonlinear response, particularly since the interaction energy between the screening cloud and the surrounding ions depends crucially on the relative positions of the density maxima and the pseudoions. The oscillations have the expected asymptotic form $r^{-3} \cos(2k_F r + \phi)$. Linear response leads to similar oscillations but with phase angle $\phi = 0$. The electron density around a proton calculated self-consistently using the nonlinear theory with exchange and correlation, and the results of Bhattacharyya and Singwi²⁵ mentioned earlier,

agree quite well. The electron density at the position of the proton obtained by these authors is about 25% larger than the value obtained by linear extrapolation to $r_s = 2$ a. u. of the results presented here. However, charge neutrality is preserved by a substantially larger first oscillation in the density than that illustrated in Fig. 1. It would be valuable to compare the two methods for larger values of r_s to confirm that the excessive charge pile-up encountered in the method of Sjölander and Stott⁷ for large r_s has been eliminated by the refinements of Bhattacharyya and Singwi²⁵

The electron-photon correlation energy and the electron density around the proton calculated using nonlinear-response theory can be substituted directly into Eq. (24) to yield a corrected value for ΔH_2 , and hence the hydrogen heat of solution can be obtained assuming that the proton resides at the octahedral interstitial position. Results are presented in Table V for ΔH_1 , E_{corr} , ΔH_2 , and the hydrogen heat of solution ΔH_H calculated using linear-response theory, the nonlinear Hartree approximation, and the full nonlinear theory including exchange and correlation.

It was mentioned earlier that linear-response theory for the screening of the proton greatly overestimates the heat of solution. Table V indicates that nonlinear Hartree theory does not bring much improvement, and this is mainly due to the underestimation of the electron-proton correlation energy. In order to obtain better agreement with experiment it is essential to include ex-

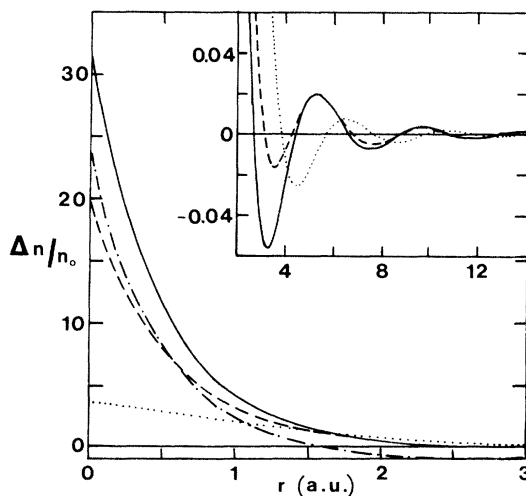


FIG. 2. Displaced electron density, $\Delta n(r) = n(r) - n_0$ in units of n_0 plotted against r (a. u.) for a proton in a uniform electron gas of mean density appropriate to Mg ($r_s = 2.642$ a. u.). Results are presented for the nonlinear theory with exchange and correlation corrections (solid line), the nonlinear Hartree theory (dash line), linear response theory (dotted line), and for the hydrogen atom (dash-dot line).

TABLE V. Summary of contributions to the hydrogen heat of solution calculated for Al and Mg along with the experimental results.

	Al	Mg
ΔH_1 (a. u.)	-0.1472	-0.1331
ΔV_p (a. u.)		
Linear theory	0.0382	0.0003
Nonlinear theory (Hartree)	0.0806	0.0294
Nonlinear (exch+corr)	0.1033	0.0447
ΔH_2 (a. u.)		
Linear theory	-0.3626	-0.3433
Nonlinear (Hartree)	-0.3708	-0.3726
Nonlinear (exch+corr)	-0.4189	-0.4469
ΔH_H (eV)		
Linear theory	1.99	2.89
Nonlinear (Hartree)	1.76	2.03
Nonlinear (exch+corr)	0.45	-0.05
Experimental	0.66 (Ref. 19)	0.25 (Ref. 20)

change and correlation corrections. The full theory underestimates the heat of solution by about 0.2 eV for Al and 0.3 eV for Mg. However the theory correctly yields a lower heat of solution for Mg unlike the linear and nonlinear Hartree approximations. The heat of solution is given as the difference of energies of about 15 eV and its value for Al and Mg is roughly 0.5 eV. In view of this cancellation the discrepancies between the full theory and experiment can be regarded as small.

VII. DIFFUSION AND POSITION OF HYDROGEN

The formulas derived for the heat of solution are valid for any position of the proton in the metal. But for the calculations presented so far it has been assumed that the proton resided at an octahedral site in both Al and Mg. This is a reasonable first assumption in view of the symmetry and the fact that the octahedral site situates the proton as far as possible from the repulsive metal ions. However, neglecting relaxation of the ions about the proton, the energy of the system as a function of the position of the proton $E(\rho_H)$ can be investigated with little additional computation. Of all the terms in ΔH_1 and ΔH_2 , given by Eqs. (20) and (24), respectively, which together with Eq. (1) give the heat of solution, only two depend on the relative positions of the proton and ions, and apart from a constant

$$E(\rho_H) = \alpha_H (\bar{\rho}_H) \frac{Z^{2/3}}{r_s} + \sum_{\vec{q} \neq 0} S(\vec{q}) n(\vec{q}) W(\vec{q}), \quad (41)$$

where α_H is the Ewald constant for the electro-

static interaction between the ions and the proton. In an earlier paper³ Popović and Stott reported calculations of the activation energies for diffusion of hydrogen in Al and Mg based on Eq. (41) and using the full nonlinear-response displaced density. In a classical model of diffusion the activation energy E_m is the height of the energy barrier over which the particle must be thermally excited in order to diffuse, and the diffusion constant is proportional to the Boltzmann factor $e^{-E_m/kT}$.

In this section results are presented for $E(\bar{\rho}_H)$ calculated for a number of positions of the proton along the principle diffusion routes, and using the nonlinear-response displaced density in Eq. (41). These results indicate the shape of the energy barrier. In the case of Al symmetry considerations indicate that the jump of the proton from one to a neighboring octahedral site must be accomplished via an intermediate tetrahedral site. In the case of Mg there are two possibilities for diffusion. The proton can jump in the direction of the c axis directly from one octahedral site to a neighboring one or, alternatively, diffusion can take place in the basal plane via an intermediate tetrahedral site. Taking the energy at the octahedral sites to be zero, $E(\bar{\rho}_H)$ has been calculated for eleven equidistant positions of the proton on the straight lines joining the different sites. The results are presented in Table VI. As reported earlier,³ in the case of Al the energy calculated for an octahedral site is lower than for a tetrahedral site, whereas for Mg the two sites have indistinguishable energies. This justifies the assumption of the octa-

TABLE VI. Energy change in eV for 11 equidistant positions of the proton on the straight lines joining adjacent sites of high symmetry. Results are given for Al for the octahedral-octahedral jump and for Mg for both the octahedral-tetrahedral jump in the basal plane and the octahedral-octahedral jump along the c axis. The heights of the energy barriers corresponding to the migration energies are given in the last row. The results of a linear-response theory are also given in parenthesis.

	Al oct \rightarrow tet	Mg oct \rightarrow tet	Mg oct \rightarrow oct
1	0.00	0.00	0.00
2	0.02	0.02	0.03
3	0.08	0.06	0.10
4	0.16	0.13	0.20
5	0.26	0.20	0.30
6	0.35	0.26	0.34
7	0.41	0.27	0.30
8	0.40	0.24	0.20
9	0.31	0.15	0.10
10	0.20	0.05	0.03
11	0.13	0.00	0.00
E_m (eV)	0.41 (1.81)	0.27 (1.61)	0.34 (1.67)

hedral site for the proton in calculating the heats of solution.

The results indicate that diffusion of the proton in Al is limited by the energy barrier around the octahedral site. The height of this barrier gives a migration energy of $E_m = 0.41$ eV, which is in good agreement with the most recently reported experimental values of³⁰ 0.47 and 0.52 eV.³¹ The migration energies have also been estimated using linear-response theory for the screening of the proton with $n^{(1)}(q)$ instead of the full nonlinear density in the second term of Eq. (41). The linear-response theory grossly overestimates the height of the potential barrier, giving for Al, $E_m = 1.81$ eV. This discrepancy again emphasizes the importance of the phase of the density oscillations to the interaction of the proton screening cloud with the surrounding ions. Another quantity relevant to the proton diffusion is the frequency of vibration $\bar{\nu}$ of the proton in the direction of the barrier about the equilibrium position. This can be estimated by fitting a harmonic-oscillator potential to the energy barrier about the octahedral position to obtain a force constant K , and then if M_p is the proton mass, $\bar{\nu} \sim (1/2\pi)(K/M_p)^{1/2}$. For Al, $\bar{\nu} \sim 1 \times 10^{13}$ sec⁻¹.

In the case of Mg no experimentally determined migration energies are available. However, recent unsuccessful attempts to quench hydrogen in Mg could be explained by fast diffusion, which would be consistent with the small calculated migration energies given in Table VI. As in the case of Al, linear-response theory overestimates the migration energies for Mg, and the results are $E_m = 1.67$ eV for the octahedral-octahedral jump and $E_m = 1.61$ eV for the octahedral-tetrahedral jump. The vibrational frequencies are estimated to be about 7×10^{12} sec⁻¹ for both types of diffusion.

In the calculations no account has been taken of relaxation of the ions around the proton. The forces acting on the neighboring ions could be calculated from the displaced electron density, and the relaxed positions of the ions then estimated using the standard methods of lattice statics. This would be a lengthy calculation and probably unprofitable in view of the small relaxation-energy contribution to the vacancy formation energy. The relaxation energies for the more confined saddle-point configurations of the proton will probably be larger than that at the equilibrium position, leading to smaller migration energies than those calculated, although this should be a small effect. The binding energy of a proton to a vacancy in Al should also be slightly affected by relaxation. The relaxation energy for the proton should be smaller when the proton is in a substitutional position than when it is interstitial, leading to a binding energy somewhat smaller than the 1.23 eV calculated

earlier using (41).³

VIII. DISCUSSION

The theory of the heat of solution of hydrogen in simple metals has been developed and applied to Al and Mg. The heat of solution was first calculated by treating the screening of the proton and the screening of the ions, described by local model potentials, using linear-response theory. The calculated values were much larger than the observed heats of solution. However, it was noted that the heat of solution can be divided into separate contributions, one from the additional electron and the other from the proton. The electron contribution should be given well by low-order perturbation theory with the ions described by a local model potential, but for the proton contribution it is necessary to go beyond linear-response theory to describe the screening of the proton. Approximately self-consistent nonlinear-response calculations of the electron density around a proton in the electron gas have been performed. The method was based on the density functional formalism of Hohenberg and Kohn¹⁰ and Kohn and Sham¹¹ with an approximate treatment of exchange and correlation. The results clearly demonstrated the inadequacy of linear-response theory for proton screening and they were used to obtain corrected values for the heat of solution which were in good agreement with experiment.

The energy of the hydrogen-metal system was investigated as a function of the position of the proton along principal diffusion routes. These results complemented the migration energies for diffusion presented previously³ and enabled an estimate of the vibrational frequency of the interstitial proton to be made. Linear-response theory of the screening of the proton was also used to estimate the migration energies and lead to gross overestimates. This was due to a poor description of the oscillations in the electron density around the proton. The phase of these oscillations plays a crucial role in the interaction energy of the electron screening cloud around the proton with the neighboring ions.

The heat of solution was calculated assuming the proton to be at an octahedral site. This is a reasonable assumption in the case of Mg since Popović and Stott³ found the octahedral and tetrahedral sites to have almost identical energies. The situation for Al requires more discussion. In this case Popović and Stott³ found that the calculated energy for the octahedral site was 0.13 eV lower than that for the tetrahedral site, indicating that the octahedral is the stable interstitial site. However, the proton at a substitutional site in Al was found to have an energy 1.23 eV lower than the octahedral site energy. This energy would be

gained by a proton falling into an existing mono-vacancy.

Assuming a value $E_v = 0.67$ eV for the vacancy formation energy,³² this implies a positive heat of solution for substitutional hydrogen of 0.1 eV which is contrary to experiment. E_B and the local density approximation for exchange and correlation is a source of error, but agreement between theory and experiment for the heat of solution for Mg and the migration energy for Al was within 0.3 eV. However first-order perturbation theory for treating the lattice is probably a poorer approximation for a substitutional than for an interstitial impurity, and errors of as much as the vacancy formation energy could be introduced into E_B . Despite these uncertainties in the calculated results we believe that proton binding to a vacancy in Al is likely.

The generally good agreement between theory and experiment suggests that the density functional formalism with the local density approximation for exchange and correlation leads to a good description of the screening of a proton in the electron gas. This method, together with the treatment of the electron-ion interaction using a model poten-

tial and low-order perturbation theory, could be used to study many other properties of hydrogen in simple metals. For instance, the interaction of the screened proton with dislocations and impurities is of great practical interest and could be treated in a straightforward manner.

The dependence of the electron-proton correlation energy for an electron gas on the mean electron density and the displaced electron densities around the proton for a range of mean densities have been investigated, and the results will appear elsewhere. Spin-polarized screening of the proton in the electron gas has not been considered here, and we do not believe that it is relevant to hydrogen in simple metals for the reasons stated earlier. However, it may be relevant to hydrogen in ferromagnetic metals and alloys and should be studied in this regard.

The screening of ions with $Z > 1$ could be studied using similar techniques to those employed here. The particular case of $Z = 2$ is of interest since experimental data³³ on He-W indicate that one or more He atoms may be trapped by vacancies paralleling the suggestion that hydrogen is trapped at vacancies in Al.

*Supported by the National Research Council of Canada.

†Present address: Xerox Research Centre of Canada Ltd., 2480 Dunwin Dr., Mississauga, Ontario, Canada L5L 1J9.

¹B. A. Kolachev, *Hydrogen Embrittlement of Non-Ferrous Metals* (Israel Program for Scientific Translations, Jerusalem, 1968).

²M. L. G. Foy, N. Heiman, W. J. Kossler, and G. E. Stronach, *Phys. Rev. Lett.* **30**, 1064 (1973).

³Z. D. Popović and M. J. Stott, *Phys. Rev. Lett.* **33**, 1164 (1974).

⁴J. Friedel, *Philos. Mag.* **43**, 153 (1952).

⁵J. S. Langer and S. H. Vosko, *J. Phys. Chem. Solids* **12**, 196 (1959).

⁶J. P. Carbotte, *Phys. Rev.* **155**, 197 (1967).

⁷A. Sjölander and M. J. Stott, *Phys. Rev. B* **5**, 2109 (1972).

⁸H. Hohenberg and W. Kohn, *Phys. Rev.* **1313**, B864 (1964).

⁹W. Kohn and L. J. Sham, *Phys. Rev.* **140**, A1133 (1965).

¹⁰Z. D. Popović, J. P. Carbotte, and G. R. Piercy, *J. Phys. F* **4**, 351 (1974).

¹¹N. D. Lang and W. Kohn, *Phys. Rev. B* **3**, 1215 (1971).

¹²Z. D. Popovic and J. P. Carbotte, *J. Phys. F* **4**, 1599 (1974).

¹³Z. D. Popović, J. P. Carbotte, and G. R. Piercy, *J. Phys. F* **3**, 1108 (1973).

¹⁴W. A. Harrison, *Pseudopotentials in the Theory of Metals* (McGraw-Hill, New York, 1970), p. 200.

¹⁵D. Pines and P. Nozières, *The Theory of Quantum*

Liquids (Benjamin, New York, 1966), Vol. 1, p. 330.

¹⁶W. M. Shyu and G. D. Gaspari, *Phys. Rev.* **170**, 687 (1968).

¹⁷K. S. Singwi, A. Sjölander, M. P. Tosi, and R. H. Land, *Phys. Rev. B* **1**, 1044 (1970).

¹⁸P. S. Ho, *Phys. Rev. B* **3**, 4035 (1971).

¹⁹W. Eichenauer, *Z. Metallkd.* **59**, 613 (1968).

²⁰Z. D. Popović and G. R. Piercy (unpublished).

²¹C. H. Hodges and M. J. Stott, *Phys. Rev. B* **7**, 73 (1973).

²²L. Hedin and B. I. Lundqvist, *J. Phys. C* **4**, 2064 (1971).

²³M. J. Stott, S. Baranovsky, and N. H. March, *Proc. R. Soc. Lond. A* **316**, 201 (1970).

²⁴K. S. Singwi, M. P. Tosi, R. H. Land, and A. Sjölander, *Phys. Rev.* **176**, 589 (1968).

²⁵P. Bhattacharyya and K. S. Singwi, *Phys. Rev. Lett.* **29**, 22 (1972).

²⁶U. von Barth and L. Hedin, *J. Phys. C* **5**, 1629 (1972).

²⁷N. H. March and A. M. Murray, *Proc. R. Soc. Lond. A* **256**, 400 (1960).

²⁸L. Fox and E. T. Goodwin, *Proc. Camb. Philos. Soc.* **45**, 373 (1949).

²⁹L. Hedin, *Phys. Rev.* **139**, A796 (1965).

³⁰Von W. Eichenauer and A. Pebler, *Z. Metallkd.* **48**, 373 (1957).

³¹S. Matsuo and T. Hirata, *Trans. Natl. Res. Inst. Met.* **11**, 22 (1969).

³²B. T. A. McKee, W. Triftshäuser, and A. T. Stewart, *Phys. Rev. Lett.* **28**, 358 (1972).

³³E. V. Kornelsen, *Radiat. Eff.* **13**, 227 (1972).